Passive silicon-on-insulator polarization-rotating waveguides

Chris Brooks
Paul E. Jessop, MEMBER SPIE
McMaster University
Department of Engineering Physics
Centre for Emerging Device Technologies
1280 Main Street West
Hamilton, Ontario, Canada L8S 4L7
E-mail: brookscj@mcmaster.ca

Henghua Deng
University of Waterloo
Department of Electrical and Computer Engineering
200 University Avenue West
Waterloo, Ontario, Canada N2L 3G1

David O. Yevick
University of Waterloo
Department of Physics and Department of Electrical and Computer Engineering
200 University Avenue West
Waterloo, Ontario, Canada N2L 3G1

Garry Tarr
Carleton University
Department of Electronics
1125 Colonel By Drive
Ottawa, Ontario, Canada K1S 5B6

Abstract. We present preliminary experimental results for silicon-on-insulator polarization rotators with asymmetric external waveguiding layers. These devices consist of a waveguide with vertical and sloped sidewalls and are fabricated using a combination of plasma and chemical etching techniques. For a device length of 3256 μm, a TE-to-TM polarization conversion efficiency of 75% was measured. *© 2006 Society of Photo-Optical Instrumentation Engineers.* [DOI: 10.1117/1.2188408]

Subject terms: silicon; polarization; integrated optics; waveguides.

Paper 050317R received Apr. 22, 2005; revised manuscript received Jul. 25, 2005; accepted for publication Aug. 17, 2005; published online Apr. 7, 2006.

1 Introduction

Polarization-rotating waveguides are the integrated optics counterparts of bulk optics wave plates. In place of material anisotropy, waveguide birefringence in an asymmetric refractive index profile is employed to manipulate the polarization state. Applications of polarization rotators include reducing the polarization sensitivity of devices in optical networks[1] and integrated optic polarization sensors.[2] As well, silicon-on-insulator (SOI) photonic devices, such as polarization rotators, can be manufactured cost-effectively, are easily integrated with silicon-based electronics, and yield strong optical confinement as a result of their high refractive index contrast.

Although the first integrated optic polarization converter designs employed several sections with periodically changing waveguide geometries,[3,4] TE↔TM mode conversion can also be achieved in a single waveguide section consisting of vertical and sloped sidewalls.[5] Such devices have been fabricated in III-V semiconductor material systems,[6,7] but have yet to be realized in SOI. In these devices, illustrated by Fig. 1, the waveguide parameters are chosen such that the effective polarization directions of the two orthogonally polarized modes are rotated at ±45 deg with respect to the lateral direction (the substrate surface).

As in a half-wave plate, when the incoming field is TE or TM polarized, the output polarization is rotated by twice the optical-axis angle after a π phase shift accumulates between the polarized modes of the asymmetric waveguide.

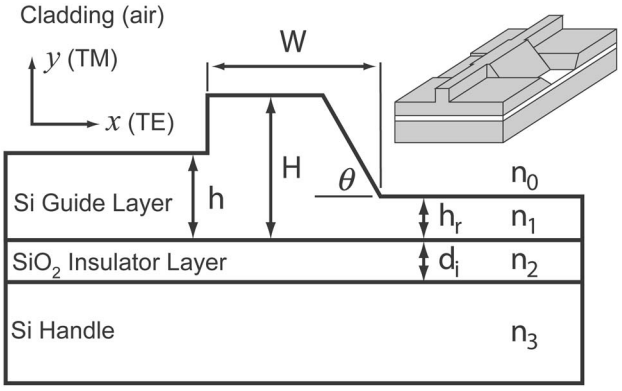


Fig. 1 SOI polarization rotator geometry for arbitrary guide-layer thicknesses. An h_r=0 polarization rotator section integrated with conventional rib waveguides is shown in the inset.

0091-3286/2006/$22.00 © 2006 SPIE

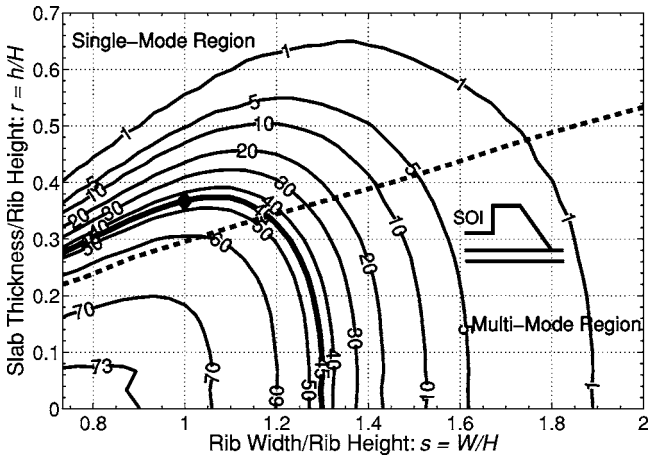


Fig. 2 Optical-axis rotation angle contours for asymmetric SOI waveguides with $h_r=0$. The contour for the desired optical-axis rotation of 45 deg is designated by a bold line, and our fabrication parameters are indicated with the symbol ♦ (Ref. 8).

This occurs at the half-beat length $L_\pi=\pi/(\beta_1-\beta_2)$, where β_1 and β_2 are the propagation constants of the two modal electric field distributions.

2 Simulation Results

Our numerical studies of polarization rotators employ a proprietary full-vectorial finite-element mode solver with mixed elements.[8] In the simulations, the sloped sidewall is angled along the (111) crystallographic plane of silicon, yielding $\theta=54.736$ deg, while the refractive indices are set to $n_1=n_3=3.48$ for the silicon layers and $n_2=1.45$ for the SiO_2 insulator layer. Further, the insulator layer thickness is $d_i=1.0$ μm, while the input vacuum light wavelength is $\lambda=1.55$ μm.

While complete TE↔TM mode conversion can be achieved if both the vertical and sloped sidewalls possess the same slab thickness ($h=h_r$ in Fig. 1), we have instead etched the sloped sidewall down to the buried insulator layer ($h_r=0$) as suggested in Ref. 8. Such a design improves the manufacturability by providing a convenient etch stop for the wet chemical used to fabricate the sloped sidewall, eliminating the need for precise etch timing. It also yields higher optical confinement and shorter device lengths than the design with $h=h_r$.

Contours for the optical-axis rotation angle as a function of slab thickness h and rib width W are shown in Fig. 2 for polarization rotators with $h_r=0$. The axes have been normalized to the guide-layer thickness H, since these contours are invariant over a wide range of thicknesses (1 to 10 μm).[8] The dashed line in the figure represents the border between single-mode (two orthogonal polarizations) and multimode operation. Since additional guided modes exhibit different half-beat lengths, optimal mode conversion requires single-mode operation.

The half-beat length can be minimized by decreasing either or both the width and the guide-layer thickness.[8] We have here employed a rather conservative waveguide geometry given by $H=4.8$ μm, $W=4.8$ μm, and $h=1.8$ μm, yielding a half-beat length of $L_\pi=2605$ μm. While the half-beat length could have been reduced to 1150 μm by employing $W=3.5$ μm, the fabrication tolerance would then be decreased. For the guide-layer thickness of $H=1.3$ μm typically used for published III-V rotators, the half-beat length for SOI rotators is around 35 to 100 μm, in comparison with device lengths of several hundred microns for III-V materials.[8] This is because of the higher refractive index contrast of SOI. We have chosen $H=4.8$ μm for this preliminary demonstration, yielding a much longer device length of 2605 μm, since the device becomes more sensitive to fabrication errors as the guide-layer thickness is decreased.[9]

The width and lateral offset of the input/output (I/O) waveguides were simulated to minimize device loss, as calculated from the overlap of the optical power of the corresponding polarized modes of the input and rotator sections. The slab thickness of the I/O waveguides was determined from the single-mode condition for SOI waveguides.[10] Accordingly, the waveguide etch depth was shallower in the I/O section than in the rotator section, resulting in a theoretical mode mismatch loss per interface of 0.75 and 0.44 dB for the TE and TM input polarizations, respectively, for a total excess loss of 1.2 dB for both interfaces. For this geometry, the optimal width of the I/O waveguides is 2.6 μm, with a slab thickness of 2.5 μm and a lateral shift of 0.2 μm between the vertical sidewalls of the I/O waveguides and the rotator section, towards the sloped sidewall.

This loss can be further reduced by using vertical tapers and/or by reducing the slab thickness of the I/O waveguides below published single-mode conditions.[10] If the slab thickness of the I/O waveguides is matched to that of the rotator section ($h=1.8$ μm), the minimized loss becomes 0.26 and 0.24 dB for the TE and TM input polarizations, for a total of 0.5 dB for both interfaces. This loss is for an optimal width of 2.5 μm, a slab thickness of 1.8 μm, and a lateral shift of 0.2 μm. This geometry would be multimode according to published single-mode conditions, since $h/H<0.5$, but appeared to be single-mode when simulated with our mode solver. More simulations using the beam propagation method are required to verify this result, for single-mode conditions for deeply etched SOI waveguides ($h/H<0.5$) have yet to be published. Therefore, the more conservative input parameters were used to guarantee single-mode operation for these preliminary results, at the expense of higher loss.

3 Experimental Results

Square pieces measuring 3.4 cm were cleaved from an 8-in. (100) SOI wafer from SEH America. The wafer was manufactured using the bond and etchback technique (BESOI) and had a guide-layer thickness of 5 μm, a 1-μm buried oxide layer, and a 725-μm base layer thickness. The wafer was lightly p-type (boron) doped with a resistivity of 20 to 30 Ω cm for the device layer and 15.5 Ω cm for the base silicon layer. An infrared-based ellipsometer was used to measure the thickness of the silicon guide layer, which was found to vary by around ±0.1 μm over the sample area. The measured thickness was used to determine the etch depth required to achieve a slab thickness of 1.8 μm, for this is the most critical device dimension.[8,9]

The vertical and sloped sidewalls of the device were

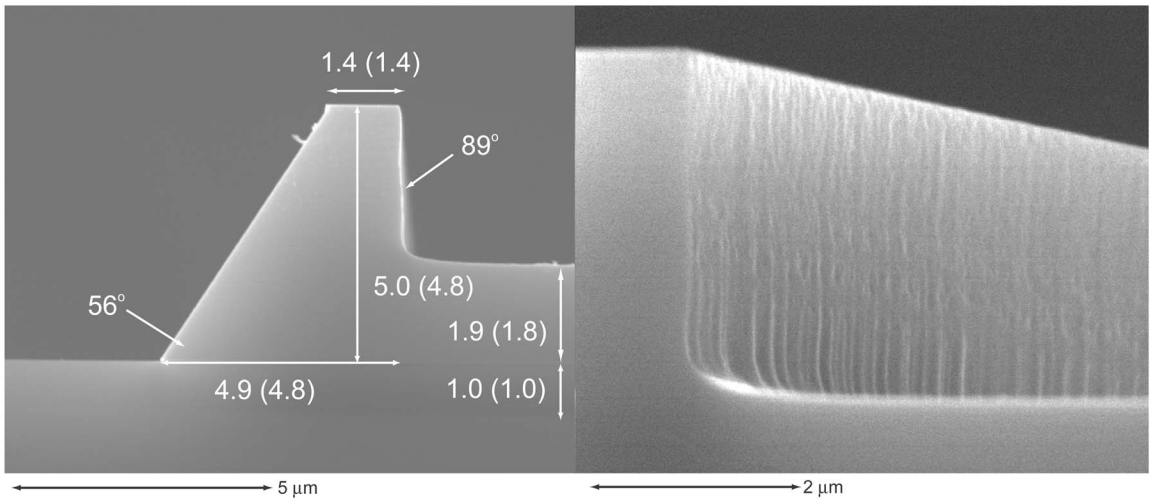


Fig. 3 A SEM cross section of the fabricated polarization rotator. The optimal dimensions (in microns) are included in parentheses. An image of the vertical sidewall roughness in the rotator section is also shown.

fabricated with dry plasma and wet chemical etching. To define the vertical sidewalls of the rotator section and the I/O waveguides, a thermally grown oxide mask was patterned using ultraviolet photolithography and reactive ion etching (RIE), with O_2 and CHF_3 as precursor gases. Because of the oxide thickness, ≈ 0.4 μm, RIE was chosen to avoid undercutting the mask. The initial alignment of the waveguides was performed using the cleaved edges of the sample to ensure the correct orientation for the wet chemical etch to be completed in a later step.

The vertical sidewalls of the rotator section and I/O waveguides were etched to a depth of 2.3 μm using electron-cyclotron-resonance reactive ion etching (ECR RIE), with SF_6 and O_2 as the precursor gases. This technique increases the etch anisotropy over that with standard RIE, noticeably improving device performance with a more vertical sidewall profile.[9] Photoresist was then applied to protect the I/O waveguides, and the vertical sidewall of the rotator section was etched an additional 0.7 μm using ECR RIE. The photoresist and oxide mask were then removed.

To define the sloped sidewall of the rotator section, a thin (≈ 0.06 μm) oxide mask was thermally grown and patterned through photolithography and HF. A thin oxide mask was sufficient for this step because of the high etch selectivity of silicon over SiO_2 with the wet chemical etchant used. The thermally grown oxide mask also reduced the roughness of the previously etched vertical sidewalls. Further, the guiding layer thickness was reduced from 5 to 4.8 μm by silicon consumption during growth of the two thermal oxide masks. It should be noted that rotational misalignment between the vertical and sloped sidewalls occurred in this step. This could have been avoided by defining both sidewalls with the same mask, and subsequently protecting one sidewall while etching the opposite wall.

The sloped sidewall was etched using a 25% tetramethyl ammonium hydroxide (TMAH) bath-heated to 60°C. TMAH exposes the (111) crystallographic planes of silicon, resulting in a sidewall that is angled by ≈ 55 deg. The silicon guide layer was etched to the buried oxide layer, which served as an etch stop. Finally, the oxide mask was removed and the samples thinned and mechanically cleaved, yielding optical-quality facets.

A range of rotator section widths were fabricated on the same sample to compensate for misalignment between the vertical and sloped sidewalls. For each misalignment, sets of 10 different rotator section lengths were fabricated, along with a single straight waveguide that was used for comparison measurements.

Scanning electron microscope (SEM) images of a cross section of the fabricated polarization rotator and the vertical sidewall roughness are presented in Fig. 3. The indicated values for the waveguide dimensions exhibit a precision of ± 0.1 μm, while the sidewall angle is accurate to ± 1 deg. The optimal design dimensions are specified in parentheses. Note that the vertical sidewall profile changes slightly along its depth, since multiple etches were required to attain the desired etch depth because an *in situ* etch-depth measurement system for the ECR RIE process was not available. These profile changes were more visible before being smoothed by the growth of the second thermal oxide mask.

To evaluate the device performance, the polarization conversion (PC) efficiency, defined as $\mathrm{PC}_{\mathrm{TE}\rightarrow\mathrm{TM}} = [P_{\mathrm{TM}}/(P_{\mathrm{TE}}+P_{\mathrm{TM}})] \times 100\%$ for a TE-polarized input, was measured. Here P_{TE} and P_{TM} are the output optical powers for the TE and TM polarization components. For comparison, the polarization conversion can be calculated using $\mathrm{PC} = 4 \sin^2\varphi \cos^2\varphi \sin^2(\pi L/2L_\pi) \times 100\%$, where φ is the optical-axis rotation and L is the length of the rotator section. The measured dimensions in Fig. 3 result in an optical-axis rotation of 41.72 deg and a 2940-μm half-beat length, yielding 95% conversion at a device length of 2605 μm. This simulated result significantly differs from the conversion efficiency measured, due to sidewall corner rounding and roughness.

Light from a 1.55-μm diode laser was TE- or TM-polarized with an extinction ratio greater than 30 dB by a

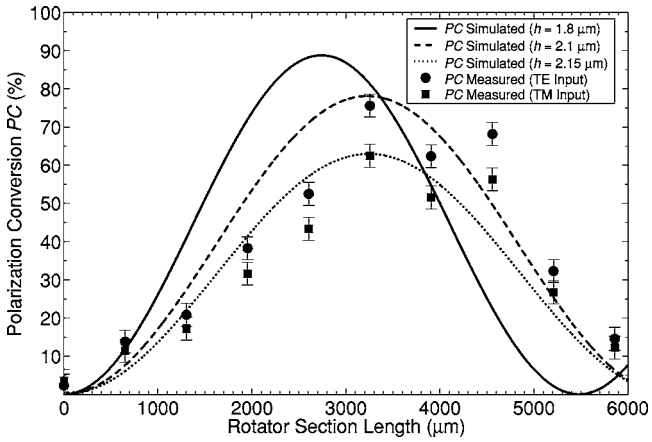


Fig. 4 Measured polarization conversion as a function of length. Simulated results are also shown for the device parameters measured in Fig. 3, with the slab thickness of the rotator section varied.

series of polarization paddles and an in-line polarizer placed before a polarization-maintaining tapered single-mode optical fiber that was used to couple light into the input waveguide. The output light was collected with a 20 $\times$ objective lens and then separated into TE and TM polarization components with a polarizing beamsplitting cube. The optical power of the desired output polarization component was measured using a photodetector.

The measured polarization conversion as a function of length for our best performing device is shown in Fig. 4. The maximum conversion efficiencies were $PC_{TE\rightarrow TM}=75\%$ and $PC_{TM\rightarrow TE}=62\%$, at a device length of 3256 μm. These measurements have uncertainties of $\pm 3\%$, obtained from the standard deviation of five measurements, each with a separate fiber alignment. The unequal conversion efficiencies result largely from the vertical-sidewall roughness, which affects each polarized mode differently. The input and output waveguides minimally affected the polarization conversion measurements, since these waveguides exhibited conversion efficiencies less than 4% in the absence of the rotating sections.

Simulations have shown that the conversion efficiency is most sensitive to changes in the slab thickness of the rotator section, while changes in the width and guide layer thickness of ± 0.2 μm result in less than a 2% decrease in conversion efficiency.[8,9] Using the device parameters measured in Fig. 3, the polarization conversion as a function of length has been calculated for various slab thicknesses ($h=1.8, 2.1, 2.15$ μm) and is included in Fig. 4. A value of $h=2.1$ μm, yielding an optical-axis rotation of 31 deg and a half-beat length of 3227 μm, best fits the measured data. This is most likely explained with the rounding of the vertical sidewall corner, which effectively increases the slab thickness.

As well, the simulated results do not match most of the measured data, due to sidewall roughness and to a change in width along the rotator section, by ≈ 0.2 to 0.3 μm, induced by the rotational misalignment between the vertical and sloped sidewalls. This difficulty could be largely eliminated by defining the top of the rotator section, and consequently both sidewalls, with a single oxide mask. The region to either the right or left of this mask is then protected, together with half of the mask, while the other side is etched. Such a procedure also ensures a constant and predictable rotator section width and eliminates any reliance on intentional misalignments as long as an alignment tolerance equal to half the width of the top of the rotator section (here ± 0.7 μm) can be achieved. Because we were unsure if our equipment could maintain this tolerance level, we applied a more conservative approach with intentional misalignments that compensated up to ± 2 μm, at the expense of rotational misalignment.

Our best-performing device exhibited an excess loss of 7.1 ± 0.5 dB for TE-polarized input light, with a loss per unit rotator section length of 0.6 ± 0.1 dB/mm, while the values for a TM polarized input field were 5.6 ± 0.5 dB and 0.5 ± 0.1 dB/mm. The excess loss was determined by comparison to the power transmitted by the rib waveguides without rotator sections. These values significantly exceed the calculated losses from the mode mismatch at the rotator section interfaces and therefore most likely are the effect of the sidewall roughness of the deeper-etched rotator section and I/O waveguide misalignment along the propagation direction. As well, the mode mismatch simulations assumed abrupt I/O interfaces, but they will in fact have pyramidlike corners near the sloped sidewall of the rotator section due to the TMAH etching along multiple crystal planes. Further simulations are required to accurately model this complicated transition.

While our simulations indicate that the conversion efficiency should vary by less than 1% over a wavelength range of 1500 to 1600 nm,[8] measurements with a tunable laser were complicated by large etalon effects that could not be removed by Fourier filtering, and we were therefore unable to verify this behavior. In the absence of proper antireflection coating of the sample facets and measurement components, it was therefore only possible to ascertain that the average conversion efficiency over the entire wavelength range of 1500 to 1575 nm coincided with the polarization conversion measured at 1550 nm to within measurement error.

4 Conclusions

We have designed and fabricated a single-section SOI polarization rotator. Its performance was limited by numerous fabrication problems, which included imprecise etch depth, corner rounding of the vertical sidewall, a change in width along the rotator section due to rotational misalignment, and sidewall roughness. Accordingly, the measured polarization conversion did not exceed 75% in any of our devices; however, we are confident that future refinements to the fabrication process should yield improved results. Indeed, preliminary tolerance study results presented in Refs. 8 and 9 that incorporate the effects of fabrication error predict conversion efficiencies of $\approx 95\%$ for industry-standard processes. Additionally, far shorter device lengths can be realized for reduced guide-layer thickness, although the sensitivity to fabrication errors is then increased.

Acknowledgments

This work was supported by the Canadian Institute for Photonic Innovations (CIPI) and by the Natural Science and Engineering Research Council of Canada (NSERC).

References

1. Y. Inoue, H. Takahashi, S. Ando, T. Sawada, A. Himeno, and M. Kawachi, "Elimination of polarization sensitivity in silica-based waveguide division multiplexer using a polyimide half waveplate," *J. Lightwave Technol.* **15**(10), 1947–1957 (1997).
2. T. Koster, P. Lambeck, and F. Horst, "Passive polarization conversion in SiON technology: structures and applications," in Proc. OSA Integrated Photonics Research (IPR) Conf. IThA1-1 (2002).
3. Y. Shani, R. Alferness, T. Koch, U. Koren, M. Oron, B. I. Miller, and M. G. Young, "Polarization rotation in asymmetric periodic loaded rib waveguides," *Appl. Phys. Lett.* **59**(11), 1278–1280 (1991).
4. J. J. G. M. van der Tol, F. Hakimzadeh, J. W. Pedersen, D. Li, and H. van Brug, "A new short and low-loss passive polarization converter on InP," *IEEE Photonics Technol. Lett.* **7**(1), 32–34 (1995).
5. V. P. Tzolov and M. Fontaine, "A passive polarization converter free of longitudinally-periodic structure," *Opt. Commun.* **127**(1–3), 7–13 (1996).
6. J. Z. Huang, R. Scarmozzino, G. Nagy, M. J. Steel, and R. M. Osgood, "Realization of a compact and single-mode optical passive polarization converter," *IEEE Photonics Technol. Lett.* **12**(3), 317–319 (2000).
7. H. El-Refaei, D. Yevick, and T. Jones, "Slanted-rib waveguide InGaAsP-InP polarization converters," *J. Lightwave Technol.* **22**(5), 1352–1357 (2004).
8. H. Deng, D. O. Yevick, C. Brooks, and P. E. Jessop, "Design rules for slanted-angle polarization rotators," *J. Lightwave Technol.* **23**(1), 432–445 (2005).
9. H. Deng, D. O. Yevick, C. Brooks, and P. E. Jessop, "The fabrication tolerance of silicon-on-insulator polarization rotators," *J. Opt. Soc. Am. A* (in press).
10. S. P. Pogossian, L. Vescan, and A. Vonsovici, "The single-mode condition for semiconductor rib waveguides with large cross section," *J. Lightwave Technol.* **16**(10), 1851–1853 (1998).

Chris Brooks received his BSc degree (2003) in medical physics from the Department of Physics and his MASc degree (2005) from the Department of Engineering Physics at the Centre for Emerging Device Technologies (CEDT), at McMaster University, Hamilton, ON, Canada. His master's thesis involved fabricating and characterizing polarization rotators in silicon on insulator (SOI). He is currently pursuing his PhD at the CEDT, focusing on three-dimensional photonic devices in SOI. During his undergraduate studies, he completed co-op work terms in biomedical optics research at the Hamilton Regional Cancer Centre and in telecommunications product development at JDS Uniphase, Ottawa, ON, Canada.

Paul E. Jessop received his BSc degree in physics from the University of Waterloo, Waterloo, ON, Canada, in 1973, and his AM and PhD degrees in physics from Harvard University, Cambridge, MA, in 1975 and 1978, respectively. He joined the Electrical Engineering Division of the National Research Council of Canada, Ottawa, ON, Canada, in 1978, where he worked in the area of laser spectroscopy of solids. Since 1981, he has been with McMaster University, Hamilton, ON, Canada, where he is currently a professor in the Department of Engineering Physics and chair of the department. His principal research interests are in the areas of integrated optics and semiconductor optoelectronic devices. He heads an active research group of about eight people, consisting of both graduate students and full-time research professionals.

Henghua Deng received his MS degree in electronics from Peking University, Beijing, China, in 2000, and his PhD degree in electrical and computer engineering from the University of Waterloo, Ontario, Canada, in 2005. He was with the National Optical Communication Laboratory, Peking University, from 1997 to 2000, working on optical add-drop multiplexers (OADMs) in all-optical networks (AONs) for Chinese National 863 High Technology and National Natural Science Foundation (NNSF) projects. His master's thesis introduced arrayed-waveguide grating (AWG) devices into OADMs and improved the crosstalk and loss performance of these devices. His PhD dissertation developed a sophisticated and versatile finite-element method (FEM) software package, including both guided-mode and beam-propagation analysis for various photonic waveguides and devices, and proposed general design procedures for asymmetric polarization rotators on both III-V and silicon-on-insulator (SOI) material systems. His current research interest includes numerical methods (e.g., the finite-element method, finite-difference method, beam-propagation method, coupled mode theory, and bending analysis) in integrated optics, silicon photonics, nanophotonics, polarization manipulating devices, and arrayed-waveguide gratings. Dr. Deng is a member of the Institute of Electrical and Electronics Engineers (IEEE) and the Optical Society of America (OSA). He is an active reviewer for various IEEE and OSA journals, including *IEEE Photonic Technology Letters, The Journal of the Optical Society of America A, The Journal of the Optical Society of America B*, and *Applied Optics*.

David O. Yevick received his PhD degree from Princeton University, Princeton, NJ, in 1977. He is a professor at the University of Waterloo, Waterloo, ON, Canada. He has written more than 120 papers involving the application of numerical and analytic procedures to optical fibers, integrated optics, and semiconductor laser modeling and is currently engaged as well in developing computational methods for optical communication system analysis. Dr.Yevick is a fellow of the Optical Society of America (OSA) and the American Physical Society (APS) and serves as an associate editor of the *Journal of the Optical Society of America A*.

Garry Tarr received his BSc in physics and his PhD in electrical engineering from the University of British Columbia in 1977 and 1981 respectively. He has served as a faculty member with the Department of Electronics, Carleton University since 1982, and currently holds the rank of professor. His general research interests are in silicon process technology and device physics. His research has recently focused on integrated optoelectronic devices in silicon-on-insulator substrates.